Molecular dynamics approach to water structure of H-II mesophase of monoolein

ARTICLE *in* THE JOURNAL OF CHEMICAL PHYSICS · FEBRUARY 2012

Impact Factor: 2.95 · DOI: 10.1063/1.3685509 · Source: PubMed

5 AUTHORS, INCLUDING:

Vesselin Lyudmilov Kolev
University of Southern California
19 PUBLICATIONS **226** CITATIONS
SEE PROFILE

Galia Madjarova
Sofia University "St. Kliment Ohridski"
24 PUBLICATIONS **253** CITATIONS
SEE PROFILE

Molecular dynamics approach to water structure of HII mesophase of monoolein

Vesselin Kolev, Anela Ivanova, Galia Madjarova, Abraham Aserin, and Nissim Garti

Citation: J. Chem. Phys. **136**, 074509 (2012); doi: 10.1063/1.3685509
View online: http://dx.doi.org/10.1063/1.3685509
View Table of Contents: http://jcp.aip.org/resource/1/JCPSA6/v136/i7
Published by the American Institute of Physics.

Molecular dynamics approach to water structure of H_{II} mesophase of monoolein

Vesselin Kolev,[1,2,a)] Anela Ivanova,[3] Galia Madjarova,[3] Abraham Aserin,[1] and Nissim Garti[1]

[1]*The Casali Institute of Applied Chemistry, The Hebrew University of Jerusalem, Edmond J. Safra Campus, Givat Ram, Jerusalem 91904, Israel*

[2]*Department of Chemical Engineering, Faculty of Chemistry, Sofia University "St. Kliment Ohridski," 1 James Bourchier Blvd., Sofia 1164, Bulgaria*

[3]*Department of Physical Chemistry, Faculty of Chemistry, Sofia University "St. Kliment Ohridski," 1 James Bourchier Blvd., Sofia 1164, Bulgaria*

(Received 30 August 2011; accepted 30 January 2012; published online 16 February 2012)

The goal of the present work is to study theoretically the structure of water inside the water cylinder of the inverse hexagonal mesophase (H_{II}) of glyceryl monooleate (monoolein, GMO), using the method of molecular dynamics. To simplify the computational model, a fixed structure of the GMO tube is maintained. The non-standard cylindrical geometry of the system required the development and application of a novel method for obtaining the starting distribution of water molecules. A predictor-corrector schema is employed for generation of the initial density of water. Molecular dynamics calculations are performed at constant volume and temperature (*NVT* ensemble) with 1D periodic boundary conditions applied. During the simulations the lipid structure is kept fixed, while the dynamics of water is unrestrained. Distribution of hydrogen bonds and density as well as radial distribution of water molecules across the water cylinder show the presence of water structure deep in the cylinder (about 6 Å below the GMO heads). The obtained results may help understanding the role of water structure in the processes of insertion of external molecules inside the GMO/water system. The present work has a semi-quantitative character and it should be considered as the initial stage of more comprehensive future theoretical studies. [http://dx.doi.org/10.1063/1.3685509]

I. INTRODUCTION

The structural properties of ternary hexagonal mesophases composed of glyceryl monooleate (GMO), tricaprylin, and water were extensively and systematically studied and the findings were reported in our numerous publications.[1–5] Garti and co-workers explored and controlled the physical properties of H_{II} mesophases to use these systems as drug delivery vehicles for biologically active peptides and proteins. The results of this structural research enabled significant expansion of the application spectrum of hexagonal lyotropyc liquid crystals, employing them for the solubilization of peptides and proteins,[6–10] into this mesophase and its utilization as a sustained drug delivery vehicle. Two model cyclic peptides, cyclosporin A (11 amino acids) and desmopressin (9 amino acids), of similar molecular weights but with very different hydrophilic and lipophilic properties, were chosen to demonstrate the feasibility of using the H_{II} mesophase.[10] In addition, cell penetrating peptides were solubilized into the H_{II} structures as model skin penetration enhancers.[11,12] Finally, larger macromolecules, the proteins lysozyme and insulin,[13,14] were directly incorporated into a GMO-based H_{II} mesophase.[15,16] However, despite the various practical applications of the H_{II} mesophases and phenomenological understanding of their physical properties, the theoretical basis for comprehending water and guest molecules behavior was scarcely studied. Noteworthy experimental studies are two reports of neutron diffraction experiments on confined water structure in cubic monoolein[17] and other lipid[18] mesophases. The authors conclude that the confinement introduces mild changes in the water structure in the sense of increased intermolecular distances and does not lead to long-range correlations among the water molecules of the order of tens of angstroms.

Molecular dynamics (MD) is the approach best suited for description of the properties of water inside GMO tubular (GMO/water) structures. Despite the applicability of this method to systems with large numbers of atoms (such as *liquid crystals*), it is not trivial to set up the computational task correctly. On the other hand, the total cost of the computations is a very important aspect. Additionally, it is not possible in practice to start simulations of the H_{II} structure only using some general considerations. One always needs an appropriate and detailed physical model, close to the real nature of the system. As far as the particular target system is concerned, there exist reports in the literature showing that the various phases of monoolein[19] and lipid/fatty acid mixtures[20] can be simulated by classical molecular dynamics.

Molecular dynamics requires a well-defined initial state, which must provide all the necessary starting information for the subsequent evolution of the simulation. If the initial state is well chosen, the model will reach equilibrium, i.e., a state

a)Electronic mail: vlk@lcpe.uni-sofia.bg.

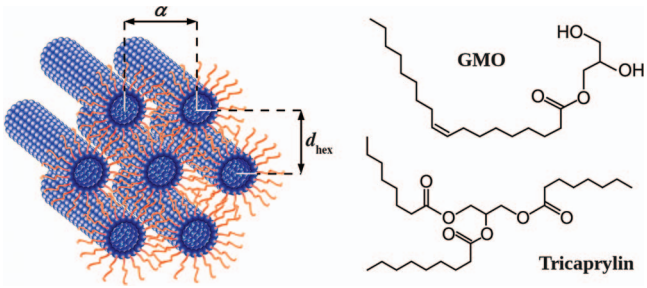

FIG. 1. Schematic representation of the inverse hexagonal (H_{II}) mesophase of monoolein and its crystal lattice parameters (left), and the structural formulas of GMO and tricaprylin (right).

close to the real studied system, in shorter time. Here we develop two interrelated methods to compose the initial state of the GMO/water structure. The first one represents a procedure for building an adequate structure of the GMO rings and tube. The recipes for calculating the geometrical parameters of a single GMO ring are well described in the literature.[21,22] Unfortunately, there are no general rules for calculating the longitudinal structure of the GMO tube, especially the distance between neighboring rings. Therefore, we propose a technique for calculating the longitudinal structural parameter based on the area of the pivotal surface of GMO molecules.[23] Our second method suggests a formal initial state of water that allows taking into account the complex geometry of the GMO tube. Generally, it is a Monte Carlo rejection sampling routine, applied for filling the cylindrical-like volume of the GMO tube with water molecules. While the first method produces a structure that remains constant during the process of simulation, the outcome of the second one is just the starting structure of water which is further subject to free dynamics. On the basis of this initial setup and the computational methods used, we expect to produce a *semi-quantitative* description of the GMO/water structure.

We used the software package GROMACS[24,25] to perform the molecular dynamics calculation, since it is reliable for simulations of solvated lipids and proteins.

II. INITIAL MODEL OF THE GMO/WATER STRUCTURE

Our initial model of the GMO/water structure can be described as a set of three general assumptions:

(i) *GMO tail geometry and the presence of tricaprylin molecules are excluded from the model*. This simplification means that in our model, GMO tubes (Figure 1) represent fixed constructions (Figure 2) composed of arranged parallel rings (Figure 2(c)) of linear GMO molecules (Figure 2(a)). The tubes are separated by layers of *vacuum* in the *x*- and *y*-direction, while they are periodic along the tube axis (*z*-direction) during the MD simulations. At first glance this may seem unjustified, but both tail geometry and the presence of tricaprylin among the tails are *taken into account implicitly in the calculations* via the pattern of building of the GMO tube (see Sec. III A). As for the GMO tube, it is proposed as a *fixed* structure and its topology cannot be affected by subsequent numerical optimization. The distribution of water molecules between GMO molecules is more influenced by the presence of hydrogen bonds and electrostatic interactions near the hydrophilic head than by the structure of tails and availability of tricaprylin. The molecules of tricaprylin are distributed among GMO tails in a way that makes their oxygen atoms inaccessible for water molecules, so we do not expect any interactions other than those already noted.

(ii) *The distance between GMO rings in the GMO/water structure (tube) could be estimated by using the pivotal surface of the lipid molecule*. In addition to (i), we have to propose a method for calculating the distance between radial planes of GMO rings. It is easy to calculate the parameters of a single GMO ring (Figure 2(b)), but there is no such simple approach when it comes to determining the distance between rings. This parameter must depend on the model used. In our model, we describe the structure of the GMO tube as composed of a sequence of mutually parallel circles with a common axis passing through their centers. Lipid molecules are arranged along the periphery of the circles. All long axes of rotation of the linear lipid molecules (obtained

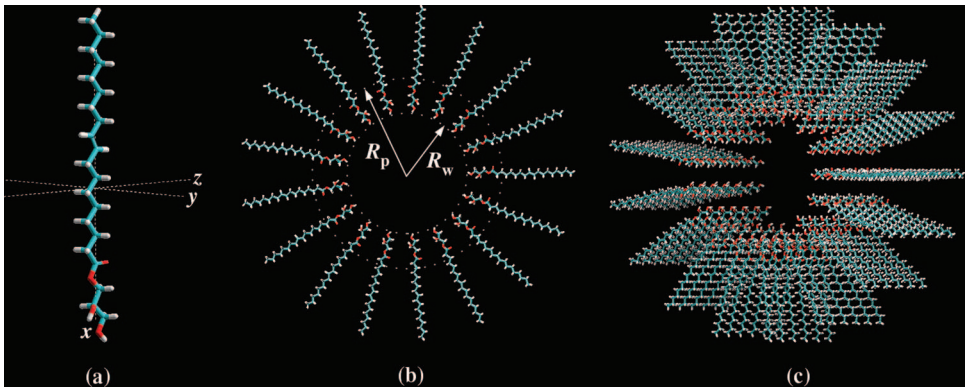

FIG. 2. (a) Structure of the GMO molecule used throughout the process of building the GMO tubes. Axis (*x*) is the longest axis of rotation. Axes (*y*) and (*z*) are presented for completeness; (b) Graphical representation of a generated GMO ring with notations of the radius of the internal empty circle and the pivotal radius R_w and R_p; (c) Skewed side view of a constructed GMO tube (see Sec. III A for detailed explanations).

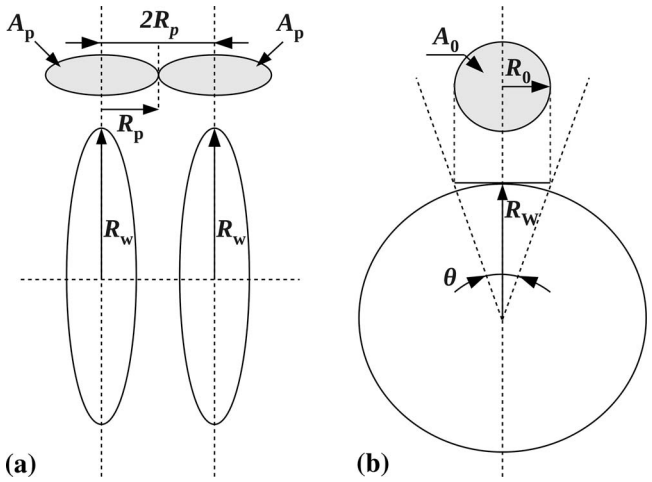

FIG. 3. (a) Pivotal surface, A_p, as a criterion for determination of the distance between GMO rings – $2R_p$ (for parameter definitions, see Sec. III A and Eqs. (10) and (11); (b) Explanation of the process of GMO ring sectorization using the sector angle θ. (see Sec. III A for details).

by fitting with the least-squares method) intersect at the center of the circle. Based on the assumptions above, we decided to use the area per GMO molecule at the pivotal plane[19] as a divider between two neighboring circles (Figure 3(a)). The pivotal plane is the plane that has a molecular cross-sectional area invariant upon isothermal bending. The position of the pivotal plane depends on the relationship between area compressibility and bending of the lipid layer. In other words, the pivotal plane position and elastic constants are specific to a particular deformation. Especially in the H_{II} phase, the pivotal plane is the surface at which the area remains constant as the curvature in the phase is changed by varying the water content. In that case, the distance between two adjacent circles is double the value of the radius of the area at the pivotal plane. The radius could be determined from an experimental dataset (see Sec. III A). The value of the distance between two neighboring circles depends on the content of both GMO and tricaprylin. Such dependence is in support of assumption (i) because it introduces yet another part of the experimental information to fix the set of parameters for the GMO structure.

(iii) *Water molecules of the GMO/water structure are considered explicitly.* The hydrophilic part of the GMO ring structure is surrounded by explicit water molecules. In our computational procedure, the *CHARMM27 force field*[27,28] is used. In addition, we propose a novel distribution method to generate the *initial* coordinates of water molecules inside the complex topology of the GMO tube (Figure 4). The method produces a hypothetical water structure without explicitly imposed hydrogen bonds, based on a randomized lattice of water oxygen atoms and the corresponding distribution of water molecules (Sec. III B). They both can be calculated on the basis of a rejection sampling Monte Carlo technique. The entire process of coordinate generation is based on the TIP3P structure model[29] of a water molecule. Here, physical instability of the initial state of water is not a problem at all, because GROMACS optimization routines provide the needed corrections, taking into account the respective interactions, including hydrogen bonds during the subsequent energy minimization step.

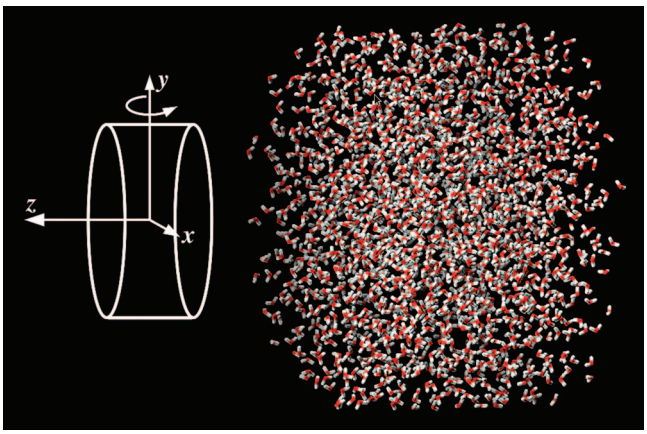

FIG. 4. Initial distribution of water molecules obtained by the Monte Carlo rejection sampling routine (see Sec. III B for details). The cylindrical volume of the distribution is rotated about the *y*-axis for a better view.

In summary, determination of the radial (transverse) structure is provided in (i) and the longitudinal structure in (ii). Initial distribution of water and the force field are provided according to (iii).

Assumption (i) eventually speeds up the entire process of numerical simulations without significant influence on the quality of the final results. It decreases the size of the system and, therefore, reduces the computational burden of the entire simulation. Figure 5 shows the *effective* part of the single ring structure, which is the subject of structure refinement. It should be noted that such a particular reduction of optimized ring size makes unnecessary the consideration of lipid tail folding. Although tail folding may lead to displacement of the theoretical axis of rotation (shown in Figure 2(a))

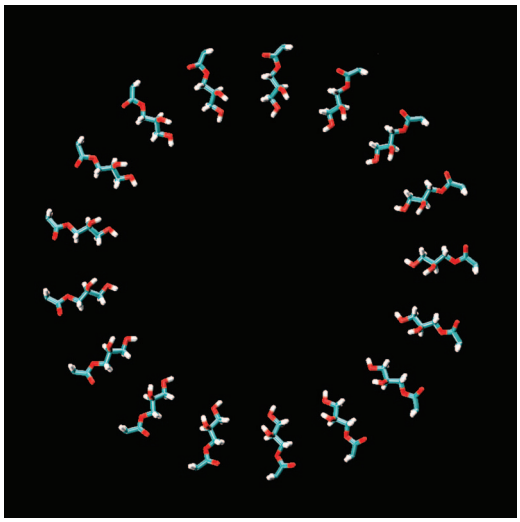

FIG. 5. The effective part of a single GMO ring, which is initially hydrated; the same structural unit is used for calculation of the positions of the GMO molecules along the ring.

out of the plane of the ring, the direction of displacement is randomly distributed. As the number of lipid molecules in the GMO tube is relatively large, it can be proved that the distribution of directions is homogeneous. Therefore, the resulting average direction of the part of the molecule that takes part in the ring structure formation process is the same as the direction in our model. Of course, this does not mean that computational routines do not consider the structure and distribution of charges along the entire length of the lipid chain. The hypothesis behind (i) says that there is no significant redistribution of charge along the lipid chains due to interactions between tails, or between tails and tricaprylin, or between tails and water molecules. In addition, it says that considerable is only the *effect of interactions* between the hydrophilic lipid head and water molecules, and between water molecules themselves. Hence, fixed geometry corresponding to all-*trans* conformation is adopted for the entire lipid tails during the MD simulations.

Assumption (ii) can be used as a core routine of the building process of the GMO tube. The first step is to generate a single GMO ring, by using (i). Next, the ring can be replicated in the third direction, creating a GMO tube with a predefined length (Figure 2(c)). So, the appropriate question now is: *what should be the length of our structure*? To answer the question, we should consider the following two preconditions:

(1) H_{II} mesophase consists of large lipid tubes – the transverse dimensions of the tubes are much smaller than the longitudinal ones (Figure 1).
(2) The effects caused by the two ends of the tube can be neglected.

Then, the answer to the question above would be: we only need an elementary unit (EU) consisting of rings and water, with finite length, that could be replicated in space to produce an infinite GMO tube. This is done by imposing periodic boundary conditions,[31] as described above. A building block of 5–6 consecutive GMO rings is chosen as sufficient for the elementary unit because a block of 5 rings contains enough lipid molecules to satisfy the hypothesis of homogeneous distribution of GMO tail directions.

III. CONSTRUCTION OF THE INITIAL STATE AND MD SETUP

Our first task was to construct the cylindrical 3D structure made of GMO molecules. The coordinates of a single GMO molecule were generated in HyperChem (Ref. 30) and then fed into a homemade program that translates and rotates the coordinates of the GMO template (see Sec. III A) to calculate the coordinate set of one GMO ring. The ring was then multiplied at predefined distances along the z-direction to form the GMO tube. In order to generate the coordinates of the water molecules inside the cylindrical shape of the GMO tube, an additional program was written following the algorithm described in Sec. III B. By concatenating the coordinate sets of the GMO tube and water, the initial coordinate set of the GMO/water elementary unit was obtained, to which periodic boundary conditions (PBC) were imposed (Sec. III C).

A. Construction of the GMO tube

The process of GMO ring construction is based on both experimental data and geometrical assumptions.[21–23] The most important parameters are the hexagonal lattice parameter of the H_{II} mesophase, α, which is related to the lattice parameter d_{hex} (Figure 1),

$$\alpha = \frac{2}{\sqrt{3}} d_{hex}, \tag{1}$$

and the respective radius of the water cylinder, R_w (Figure 3(b)), which depends on α as given by the equation

$$R_w = \alpha \sqrt{\frac{\sqrt{3}}{2\pi}(1-\phi_l)}, \tag{2}$$

where ϕ_l is the lipid volume fraction. The surface area per GMO molecule at the Luzatti interface, A_0 (Figure 3(b)), is evaluated by the formula[21,22]

$$A_0 = \frac{4\pi R_w V_l}{\sqrt{3}\alpha^2 \phi_l}. \tag{3}$$

Here, V_l is the geometrical volume of the GMO molecule (628.61 Å^3). The next parameter needed is the number of GMO (lipid) molecules in the ring – N_l. To find its value, we must sectorize the circle with radius R_w into N_l equal sectors with angle θ. The angle could be estimated by using A_0,

$$A_0 = \frac{4\pi R_w V_l}{\sqrt{3}\alpha^2 \phi_l} = \pi R_0^2. \tag{4}$$

Hence, the radius of the bottom of the cylinder base could be expressed as

$$R_0 = \sqrt{\frac{4 R_w V_l}{\sqrt{3}\alpha^2 \phi_l}}. \tag{5}$$

Following the geometrical approach shown in Figure 3(b), it is easy to estimate the sector angle θ by using Eqs. (2) and (5),

$$\theta = 2\arctan\left(\frac{R_0}{R_w}\right) = 2\arctan\left(\sqrt{\frac{4V_l}{R_w\sqrt{3}\alpha^2\phi_l}}\right). \quad \text{(predictor)}. \tag{6}$$

Now it is possible to calculate the maximum value of N_l by using the maximum possible number of circle sectors with angle θ,

$$N_l^* = \frac{2\pi}{\theta}. \quad \text{(predictor)}. \tag{7}$$

Unfortunately, due to transcendence of π and other factors, it is impossible to obtain an integer value of N_l using only Eq. (7). To produce an integer value, we have to take only the integer part of the result

$$N_l = \text{int}\left(N_l^*\right) = \text{int}\left(\frac{2\pi}{\theta}\right). \quad \text{(corrector)}. \tag{8}$$

Hence, we need to correct the angle value by using the corrected value, N_l,

$$\theta_{eff} = \frac{2\pi}{N_l}. \quad \text{(corrector)}, \tag{9}$$

TABLE I. Parameters of the studied systems at various water weight fractions and GMO/tricaprylin weight ratios[26] (dilution line) at $t = 25$ °C: the hexagonal lattice parameter of the inverse hexagonal phase, α (Eq. (1)); the lipid volume ratio, ϕ_l; the radius of the water cylinder, R_w (Eq. (2)); area at the Luzatti interface, A_0 (Eq. (3)); the number of lipid molecules in a GMO ring, N_l (Eq. (8)); the effective sector angle, θ_{eff} (Eq. (9)), and the radius of the pivotal area, R_p.

C_w (wt. %)	Dilution line	α (Å)	ϕ_l	R_w (Å)	A_0 (Å^2)	N_l	θ_{eff} (deg)	R_p (Å)
10	90/10	45.05	0.90	7.29	18.10	9	40.00	21.66
20[a]	95/5	54.70	0.81	12.55	23.65	14	25.71	26.55
20	90/10	54.40	0.81	12.48	23.78	14	25.71	26.40
25[a]	90/10	56.20	0.76	14.44	27.42	15	24.00	27.42
25[a]	95/5	59.70	0.76	15.34	25.81	17	21.18	29.13

[a]Subject of MD simulations with GROMACS.

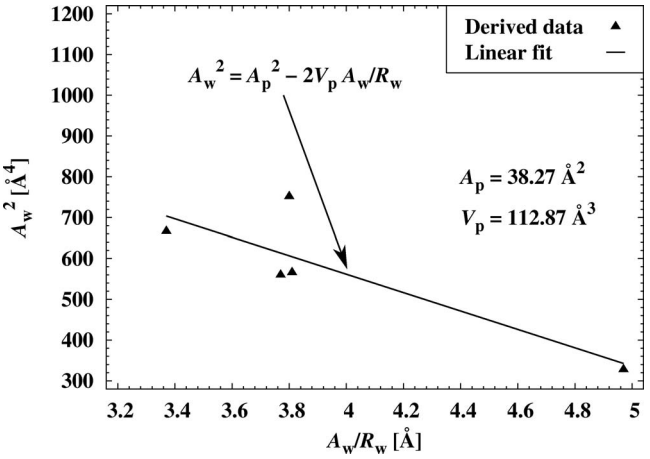

FIG. 6. The pivotal area and the pivotal volume estimation by fitting an appropriate dataset with Eq. (11). The values of R_w and A_w are taken from Table I.

and use only the *effective sector angle,* θ_{eff}, in our computational routines. Table I contains the set of calculated R_w, A_0, N_l, and θ_{eff} for the particular systems studied.

To compute the coordinates of a single GMO ring, we have to use (i) and Eq. (9), and place the coordinates of the lipid molecules at the periphery of the so-formed circle. The process of placement consists of consecutive coordinate translation (R_w) and rotation (θ_{eff}). An additional constraint imposed is that the rotation axes of the molecules have to lie in the plane of the circle.

GMO tube coordinates are the merged set of GMO rings coordinates, as (ii) claims. To build the set, we have to know the distance between two neighboring circle planes, $d_p = 2R_p$ (Figure 3(a)). Its estimation is possible by means of the *pivotal area*[22,23] of a GMO molecule, A_p,

$$d_p \equiv 2\sqrt{\frac{A_p}{\pi}}. \tag{10}$$

We can calculate A_p by using the values of R_w and A_0, summarized in Table I, and the following equation:[22]

$$A_0^2 = A_p^2 - 2V_p\frac{A_0}{R_w}. \tag{11}$$

From the corresponding best linear fit (Figure 6), $A_p = 38.27$ Å^2 and $V_p = 112.87$ Å^3. Thus, $d_p = 6.98$ Å. The last column of Table I presents the calculated values of the *pivotal radius*,[22,23] R_p, for completeness.

Now the GMO tube coordinate set (Figure 2(c)) can be calculated since all required parameters are known.

B. Construction of the initial water structure

Our most important task is to generate (draw) the coordinates of water molecules inside the GMO ring structure, i.e., to generate the distribution of water within the non-trivial shape of the cylinder, for which there is no routine procedure implemented in the available MD codes. The main obstacle in doing this is the fact that water is distributed not only inside the empty GMO tube, but also among the GMO heads. It is easy to calculate that the length of the hydrophilic head is about 7.8 Å, so the radius of the water phase must be at least $R_w + 7.8$ Å. However, such a conclusion imposes a set of very complex requirements and limitations on the algorithm for coordinate generation of water molecules. It has to take into account the heads of GMO submerged in water and their volumes have to be excluded from the volume of the water cylinder, not only as a value but also as a set of coordinates. An accurate possibility to do so is to construct an adaptive algorithm on the basis of a rejection sampling technique and to draw water molecules only if they satisfy the rules of rejection. Thus, we can obtain the real volume of the water structure and it should be regarded as the *accessible volume* for water molecules, V_w.

For the purpose, we need to know the temperature and respective densities of water and GMO. The temperature, at which our system is investigated, is $t = 25$ °C, the densities of water and GMO are $\rho_w = 0.997048$ g cm^{-3} and $\rho_{GMO} = 0.942$ g cm^{-3}, respectively.[21] Then, we have to calculate the total number of water molecules, N_w,

$$N_w = \text{int}\left(\frac{N_A\rho_w V_w}{M_w} \times 1.10^{-24}\right). \tag{12}$$

Here N_A is Avogadro's constant (mol^{-1}) and M_w is the molecular weight of water (g mol^{-1}). The multiplier 1×10^{-24} is a dimension correction. However, the value of V_w is yet unknown. To calculate it, we should represent the accessible volume as a difference of two volumes:

$$V_w = V_{w,c} - V_{w,s}. \tag{13}$$

In Eq. (13), $V_{w,c}$ is the geometric volume of a cylinder with radius $R_w + 7.8$ Å and length h,

$$V_{w,c} = \pi(R_w + 7.8\text{Å})h, \tag{14}$$

$V_{w,s}$ is the volume of the hydrophilic head of the GMO molecule and it cannot be regarded as a geometrical volume corresponding to a simple shape because of its physical meaning. Therefore, we need an appropriate physical model to calculate $V_{w,s}$. In our case, it is reasonable to calculate $V_{w,s}$ using the *van der Waals radii* of the atoms.[33] Utilization of the surface-accessible area[34] is inapplicable in the situation because it increases the calculated values significantly and

TABLE II. List of rejection sampling rules used to determine the coordinates of oxygen atoms in a randomized water lattice and to fix the positions of the hydrogen atoms of water molecules. See Sec. III B for details.

Intermolecular neighbors (atoms)	Minimal length before rejection (Å)
O(water)–O(water)	2.70
O(water)–O(GMO)	1.50
O(water)–H(GMO)	1.97
O(water)–H(water)	1.97
O(water)–C(GMO)	1.50
H(water)–O(GMO)	1.97
H(water)–C(GMO)	1.20
H(water)–H(GMO)	1.00

does not take into account the proposed rejection sampling technique.

The above assumptions look largely reasonable, but in practice it is impossible to produce good results only by generating water molecule positions up to the upper limit of the hydrophilic head. For better estimates, we need to extend the water cylinder up to the fourth carbon atom in the GMO tail. This technique might prevent the depletion of water during the process of optimization.

There is another enhancement and it affects the value of water density. It is impossible to use its tabulated values in Eq. (12). The initial water density of the system should be considered as a fit parameter (see Sec. III C for details) and has to be optimized. It was chosen such that the axial periodicity of the GMO tube, i.e., equal distance between the GMO rings, is maintained also between the elementary unit and the periodic images.

Once we know the total number of water molecules, we can start computing their distribution inside the accessible volume of the water structure. The computations can be done only by means of a well-designed rejection sampling routine. Such a routine must define all the criteria for acceptance or rejection of tested coordinates of water molecules. The core of the routine is a (coordinate) model of a water molecule. It uses the TIP3P model:[29] length of H–O bond – 0.9584 Å, angle – 104.45°. As a major parameter of the water distribution, we take the minimum distance between oxygen atoms in water at $t = 25$ °C – 2.7 Å. By means of this value, it is easy to set a rejection sampling rule and build an initial structure of water centers in the form of a randomized 3D lattice of oxygen atoms. Therefore, our first step is to generate the coordinates of the oxygen atoms of the water molecules by using a 3D random vector generator and the appropriate rejection rule. There is no need to draw the hydrogen atoms at this stage. They have to be placed in the system coordinate set after fixing the oxygen lattice and their positions are subject to another (different) rejection sampling routine, which performs rejection or acceptance of hydrogen positions during the process of 3D random rotation of a water triangle around its oxygen atom. See Table II for the complete list of used rejection sampling rules.

The core of the coordinate generation routine must be a fast and well-designed generator of 3D random vectors in cylindrical coordinates. To speed up the process of random vector generation, we ought to use an efficient algorithm without internal rejection sampling. Its schema is relatively simple. We just need a 1D uniform random generator (we used the Python random() function). First, call the 1D generator once and get the random distributed value of x within $[-R, R]$. Second, call the 1D generator within [0, 1), get another random distributed value – Ω, and compute the result of the function sign(Ω), defined as follows:

$$\text{sign}\,(\Omega) = \begin{cases} -1, \Omega \in [0, 0.5) \\ +1, \Omega \in [0.5, 1) \end{cases}. \tag{15}$$

Finally, calculate the y-coordinate of the 2D random vector through the formula

$$y = \text{sign}\,(\Omega)\sqrt{R^2 - x^2} \tag{16}$$

and extend the generated 2D random vector into the 3D one by calling again the 1D random generator – this time within the range $[0, h]$. The coordinates of the newly generated 3D random vector could be added to the vector coordinate array if they satisfied the rejection sampling rules. The set represents homogeneously distributed 3D random vectors inside the volume of a cylinder with radius R and length (height) h.

Figure 4 shows the generated water structure inside the cylinder. To understand better the properties of the distribution, we can calculate the probability mass function (PMF) and the cumulative distribution function (CDF) of the proposed oxygen positions. Figure 7 shows the PMF of all the distances among 1514 oxygen atoms of the water molecules (not only between oxygen atoms of neighboring water molecules). The oxygen lattice is inside the cylindrical volume and there are no submerged GMO heads therein ($R_w = 12$ Å, $h = 100$ Å). According to the maximum value, the most probable distance between two arbitrary oxygen atoms is about 19 Å. The value of the minimum determines the distance below which oxygen atoms might be regarded as neighbors – about 4.2 Å. Hence, the most probable distance between neighbors is between 2.75 Å and 4.2 Å. The average number of neighbors of each oxygen atom may be calculated by using the CDF (Figure 7) and it is about 6.

To complete the coordinate generation of the entire GMO/water system, the coordinate sets of the GMO tube and water molecules have to be merged and the result is represented by the coordinate set of the initial GMO/water structure in Figure 8.

C. MD setup

The dimensions of the used periodic box were 120 × 120 × 37.724 Å. The box was chosen large enough in the x and y direction to: (i) host all studied GMO tubes with various ring radius (Table I) and (ii) eliminate the periodicity in these two dimensions. Using a vacuum layer of minimum 40 Å thickness between two neighboring tubes in the radial direction (xy) is equivalent to eliminating the interactions between them. Due to the imposed *NVT* ensemble,[32] the dimensions of the box are kept fixed during the MD simulation. Since the aim is to obtain only the water structure, the dynamics of

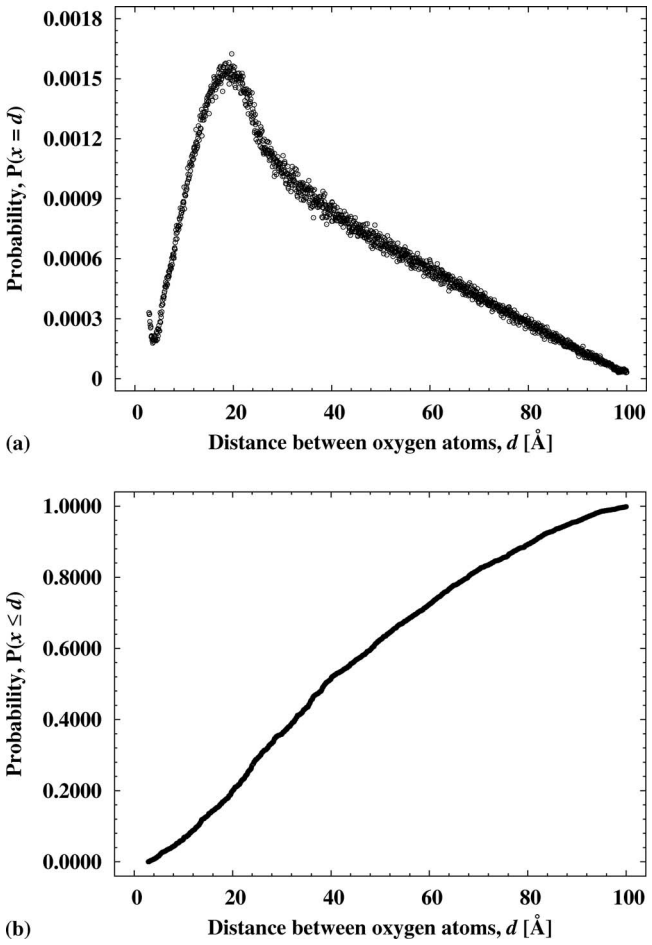

FIG. 7. (a) Probability mass function and (b) cumulative distribution function of the distances between 1514 oxygen atoms of water molecules inside the water cylinder of a GMO/water structure. The oxygen lattice forms a cylindrical volume with no submerged GMO heads within (R_w = 12 Å, h = 100 Å) (see Sec. III B for explanations).

the GMO molecules has to be excluded by fixing their atom positions. This was done by imposing a harmonic restraining potential (k = 1000 kJ/mol per atom) on the non-hydrogen atoms of GMO acting throughout the entire MD runs.

The MD simulations consisted of the following four subsequent stages: energy minimization of the GMO/water structure at 0 K, subsequent heating to 298.15 K (25 °C) over a period of 100 ps, relaxation for 1000 ps, and a 10 ns production stage. Electrostatic interactions were evaluated by the particle mesh Ewald method (PME) scheme[35] with a cutoff of 14 Å (with a switching function turned on at 12 Å) on the direct part of the sums. A switched cutoff of 12 Å, the switching function turned on at 10 Å, was applied for the non-bonded interactions. LINCS (Ref. 24) and SETTLE (Ref. 36) were used for fixing the length of the H-containing bonds of GMO and water, respectively. The constant temperature was maintained by the Berendsen thermostat.[37] The equilibration of the simulations was determined from convergence of the potential energy. The average values and the fluctuations of the temperature and pressure were monitored, too. The production trajectory was analyzed in terms of: (1) density distribution in axial and radial directions, (2) radial distribution functions (RDFs), and (3) distribution of hydrogen bonds. All procedures were done as implemented in GROMACS 4.5.3. Unfortunately, the GROMACS utilities g_hbond, g_density, and g_rdf do not support dynamic preconditions and vector selections to match dynamically only those water molecules that are located inside the cylinder and not among the GMO heads. To process the results, we created an additional program and analyzed 10 000 frames, evenly extracted (at intervals of 1 ps) from the production trajectory. Then, the script creates an index file for each frame that matches only the water molecules inside the cylinder. We used the generated index files as input for g_hbond, g_density, and g_rdf. As mentioned, we used PBC as a predictor-corrector schema to calculate the optimal initial density of water for each of the studied systems. How does this schema work? If we use PBC, GROMACS creates an infinite GMO tube by replicating the coordinates of the input elementary unit (Figure 8) along the z-axis. Therefore, the tube can be considered as created of an infinite number of EUs. Let us generate an initial water structure using some value of the density (e.g., 0.68 g cm^{-3}), then fill in the respective number of water molecules calculated as described above (Sec. III B) and apply the PBC. When finished, we check the distance between the last GMO ring of a previous GMO elementary unit of the tube and the first one of the next GMO elementary unit. If the distance coincides with that between two neighboring rings within the elementary unit, then the proposed initial density is considered to be correct. Otherwise, the initial density is changed and another set of water molecules is generated. Although the proposed schema is applicable in our case, it has no universal relevance and should be used very carefully.

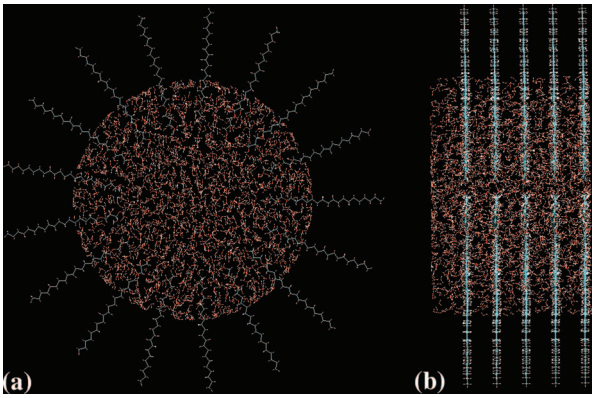

FIG. 8. Front (a) and side (b) visualization of the coordinate set of the initial structure of a GMO/water system. The first GMO ring of the structure is removed to satisfy the PBC requirements.

IV. RESULTS AND DISCUSSION

MD simulations were performed for all systems in Table I marked with an asterisk, according to the procedure described in Sec. III C, and an illustrative example of the obtained structures is displayed in Figure 9. The particular systems addressed were selected due to their large radius of the water cylinder, R_w, and the corresponding possibility of external molecules "penetration" inside the water channel. The remaining two systems in Table I are used only during

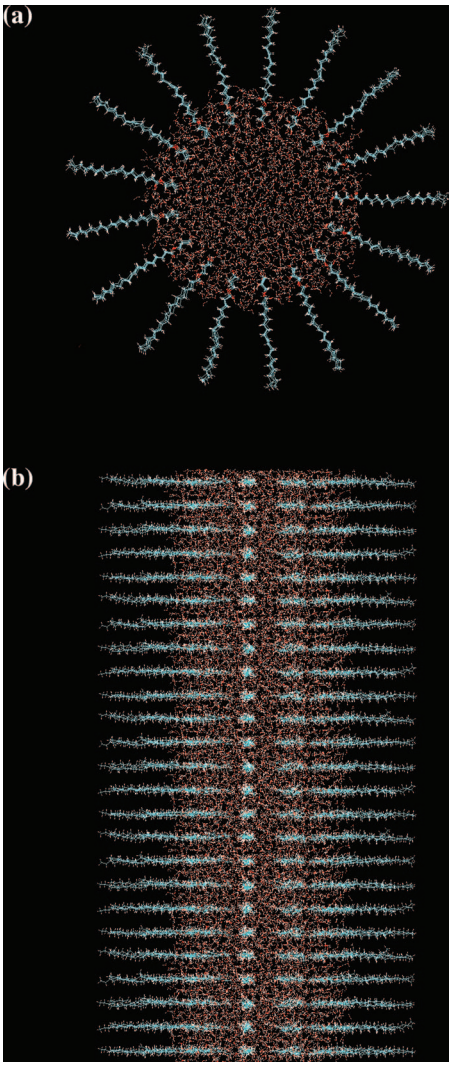

FIG. 9. An illustrative example of the GMO/water structure obtained after the MD simulation of system with $N_l = 17$ (Table I): (a) radial view; (b) side view with periodic boundary conditions applied. Due to the careful initial arrangement of water molecules and their quantity (fitting of water density), there is no depletion or significant excess of molecules.

the process of obtaining the value of the pivotal radius, R_p, as well as for illustrative purposes.

Figure 10 represents the length distribution of hydrogen bonds between water molecules and GMO and among the water molecules themselves, for all studied systems. In both cases, the most probable length of the hydrogen bonds is about 1.87–1.89 Å. According to Jeffrey,[38] the obtained distance describes hydrogen bonds inside the GMO/water system as *moderate and mostly electrostatic*. The similarity in the distributions of the two types of hydrogen bonds implies that the hydrogen bonding affinity of the hydroxyl groups from the GMO head is very close to that of the water molecules. This observation is in agreement with the results of Lee, Mezzenga, and Fredrickson.[39,40] The well-expressed tail of the curve in Figure 10 shows that long hydrogen bonds ($d > 2$ Å) also have non-zero population. This is an indication about the existence of structural anisotropy, most probably close to the surfactant heads. The calculated number of hydrogen bonds per GMO head is about 5.

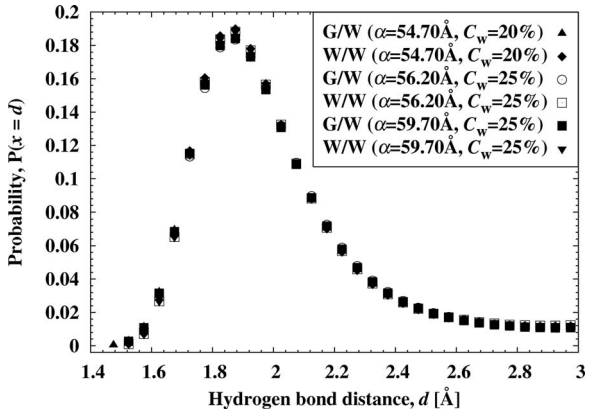

FIG. 10. Probability mass function of hydrogen bond distances between the GMO and the water molecules (G/W) and between the water molecules themselves (W/W).

The obtained transverse (radial) and longitudinal distributions of water density inside the cylinder are shown in Figure 11. The longitudinal distribution (Figures 11(b), 11(d), and 11(f)) has periodicity corresponding to the position of the GMO rings. The reason for that behavior is the hydration of the hydrophilic heads of GMO – it increases the water density between the lipid molecules, where the hydroxyl and carboxyl groups are located. The density reaches values close to the bulk density of water only at the maxima, while below the surfactants water has somewhat lower density. Increasing the tube radius has no regular effect on the water density distribution. The maxima in the smallest cylinder correspond to highest density but so do the minima. This means that in this system there are more water molecules close to the surfactants. However, as a result the last GMO ring is not as hydrated as the other ones. In the two tubes with larger radii, the water distribution along the tube axis is much more homogeneous reaching identical maximum values of $\sim$1 g/cm^3. The minimum density is a bit higher for the larger system, which might imply that the hydrophilic heads are better hydrated there.

The radial distribution of water density across the cylinder (Figures 11(a), 11(c), and 11(e)) shows that water has ordered structure deep in the cylinder volume. The estimated radial length of the peak sequence is about 6 Å in all studied systems. This means that protrusion of structuring does not depend materially on the size of the cylinder. The same is not true about the relative density close to the vicinity of the cylinder. In the two larger systems, the last peak is the highest. This corresponds to concentration of water molecules close to the surfactants. In the smallest system, however, this peak is much lower relative to the other ones. This can have a twofold meaning: either the water in this model is not sufficient to solvate properly the GMO heads or there is some frustration in the water structure due to the confined volume. The first alternative can be ruled out because tests were made with various number of water molecules (see above) until the optimum value was found. This leaves the possibility that the irregularities in the water structure result from insufficient space in the smallest cylinder. It should be noted, however, that the density distribution is not a very reliable source of information about the particulate liquid structure. Hence, we need to obtain some

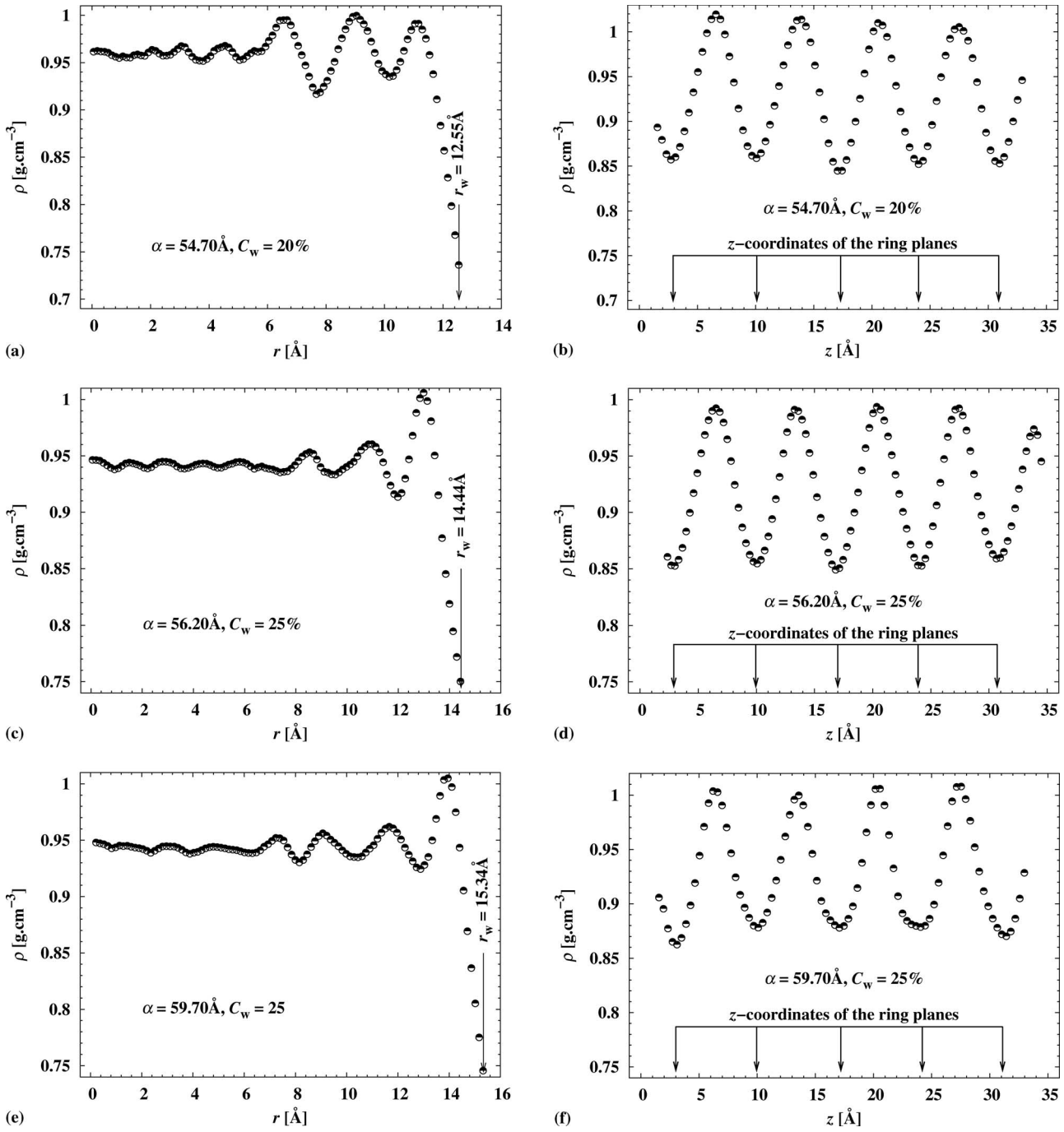

FIG. 11. Distribution of water density across the three cylinders with different radii: (a), (c), and (e) – radial distribution (*xy*-coordinates); (b), (d), and (f) – longitudinal distribution (*z*-coordinate). All *z*-positions of the planes of the GMO circles are marked with arrows.

additional information to prove or reject the observed results. As such, we can use the RDFs.

RDFs are widely used for studying the structure of liquids.[41] They are more accurate than the density distribution when molecular packing is concerned. Figure 12 shows the calculated radial distribution function of the distance between the hydroxyl oxygen atom of the GMO molecule nearest to the water cylinder, which plays the role of a center for the RDF, and oxygen atoms of the water molecules inside the cylinder. The results confirm the conclusion from the density analysis discussed above. There is a relatively well-defined water structure 7–8 Å away from the hydroxyl oxygen atom. Is should be mentioned that due to definition particularity, the obtained distance should be corrected by the difference between the radius of the hydroxyl oxygen atom and the radius of the water cylinder, which is about 2.37 Å. If that correction is applied, we get the distance of about 6 Å, which is in good agreement with the above result from the water density analysis. The three studied systems are characterized by broad peaks of the radial RDF. This means that, although there is long-range order within the water in the cylinder, the water molecules are not packed in a crystalline-like pattern

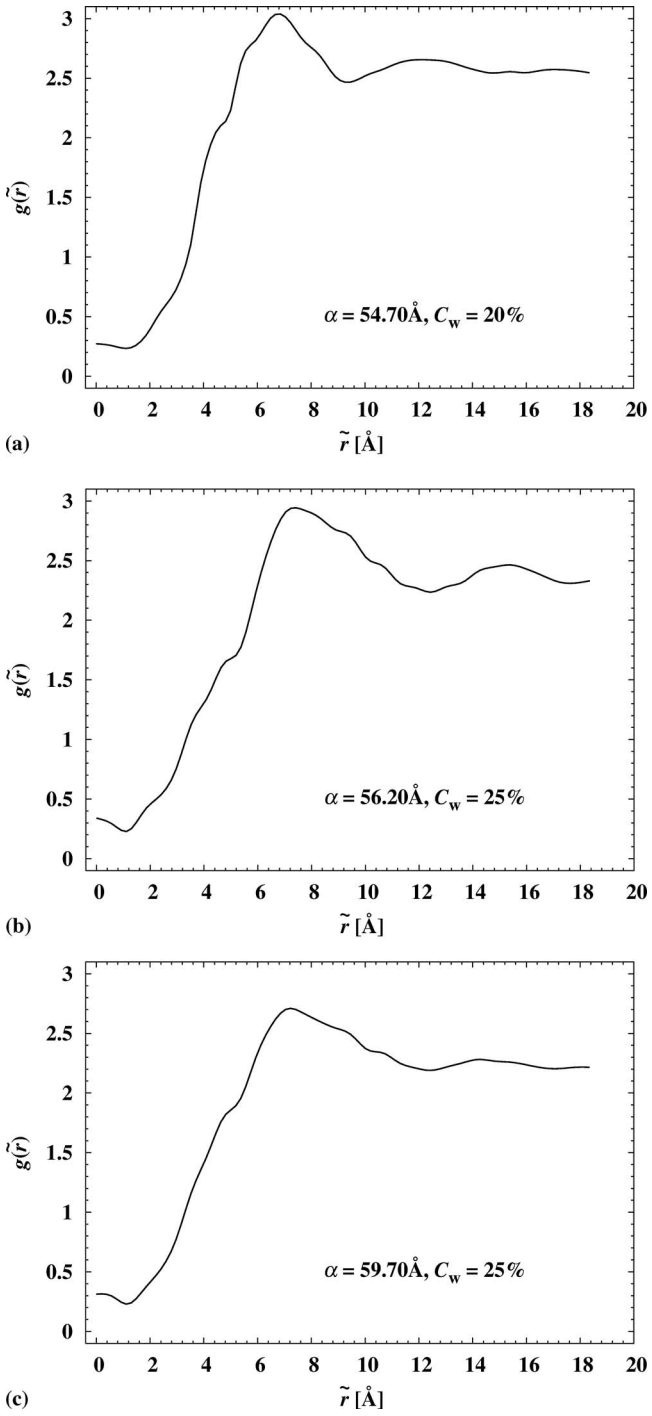

FIG. 12. Radial distribution function, $g(\tilde{r})$, of the distance between the hydroxyl oxygen of GMO, $\tilde{r}$, directed towards the water cylinder, and oxygen atoms of the water molecules. Only the *xy*-component of the distance is used.

around the surfactant heads. Thus, no definite solvation shells of GMO can be discriminated.

V. CONCLUSIONS

The work consists of two parts. First, a novel model for water distribution into the cylindrical shape of monoolein tubes is developed and implemented. Next, molecular dynamics simulations are performed in order to study the structure and dynamics of the aqueous subphase in the constrained cylindrical volume. The data are analyzed in terms of intermolecular arrangement of the water molecules.

The length distribution of the hydrogen bonds formed between GMO and water shows existence of fairly strong hydrogen bonding interaction between the two subsystems. The similar average length of the GMO-water and water-water hydrogen bonds signifies competitive hydrophilicity of GMO heads and water molecules. Both water density profiles and radial distribution functions evidence the existence of structural order of the aqueous subphase around the GMO hydrophilic heads. Water structuring protrudes down to ~6 Å in the water volume without forming definite crystalline-like arrangements. All these render the aqueous environment within monoolein tubes different from that of bulk water, which might be a driving force for the insertion of "foreign" molecules into the H_{II} mesophase of the GMO/water system, which is the target of future studies.

[1]I. Amar-Yuli, D. Libster, A. Aserin, and N. Garti, Curr. Opin. Colloid Interface Sci. **14**, 21 (2009).
[2]I. Amar-Yuli, E. Wachtel, E. Ben Shoshan, D. Danino, A. Aserin, and N. Garti, Langmuir **23**, 3637 (2007).
[3]I. Amar-Yuli, E. Wachtel, D. Shalev, H. Moshe, A. Aserin, and N. Garti, J. Phys. Chem. B **111**, 13544 (2007).
[4]I. Amar-Yuli, E. Wachtel, D. Shalev, A. Aserin, and N. Garti, J. Phys. Chem. B **112**, 3971 (2008).
[5]I. Amar-Yuli, A. Aserin, and N. Garti, J. Phys. Chem. B **112**, 10171 (2008).
[6]I. Amar-Yuli, D. Azulay, T. Mishraki, A. Aserin, and N. Garti, J. Colloid Interface Sci. **364**, 379 (2011).
[7]M. Cohen-Avrahami, A. Aserin, and N. Garti, Colloids Surf. B **77**, 131 (2010).
[8]M. Cohen-Avrahami, D. Libster, A. Aserin, and N. Garti, J. Phys. Chem. B **115**, 10189 (2011).
[9]D. Libster, A. Aserin, E. Wachtel, G. Shoham, and N. Garti, J. Colloid Interface Sci. **308**, 514 (2007).
[10]D. Libster, P. Ben Ishai, A. Aserin, G. Shoham, and N. Garti, Langmuir **24**, 2118 (2008).
[11]D. Libster, P. Ben Ishai, A. Aserin, G. Shoham, and N Garti, Int. J. Pharm. **367**, 115 (2009).
[12]D. Libster, A. Aserin, D. Yariv, G. Shoham, and N. Garti, J. Phys. Chem. B **113**, 6336 (2009).
[13]D. Libster, A. Aserin, and N. Garti, J. Colloid Interface Sci. **356**, 375 (2011).
[14]T. Mishraki, D. Libster, A. Aserin, and N. Garti, Colloids Surf. B **75**, 47 (2010).
[15]T. Mishraki, D. Libster, A. Aserin, and N. Garti, Colloids Surf. B **75**, 391 (2010).
[16]T. Mishraki, M. F. Ottaviani, Al. Shames, A. Aserin, and N. Garti, J. Phys. Chem. B **115**, 8054 (2011).
[17]C. Czeslik, E.-M. Pospiech, and R. Winter, Phys. Chem. Chem. Phys. **2**, 1621 (2000).
[18]C. Czeslik and R. Winter, J. Mol. Liq. **98**, 283 (2002).
[19]S.-J. Marrink and D. P. Tieleman, Biophys. J. **83**, 2386 (2002).
[20]V. Knecht, A. E. Mark, and S.-J. Marrink, J. Am. Chem. Soc. **128**, 2030 (2006).
[21]C. V. Kulkarni, W. Wachter, G. Iglesias-Salto, S. Engelskirchen, and S. Ahualli, Phys. Chem. Chem. Phys. **13**, 3004 (2011).
[22]J. M. Seddon, R. H. Templer, N. A. Warrender, Z. Huang, G. Cevc, and D. Marsh, Biochim. Biophys. Acta **1327**, 131 (1997).
[23]D. Marsh, Chem. Phys. Lipids **164**, 177 (2011).
[24]D. van der Spoel, E. Lindahl, B. Hess, G. Groenhof, A. E. Mark, and H. J. Berendsen, J. Comput. Chem. **26**, 1701 (2005).
[25]B. Hess, C. Kutzner, D. van der Spoel, and E. Lindahl, J. Chem. Theory Comput. **4**, 435 (2008).
[26]I. Amar-Yuli and N. Garti, Colloids Surf. B **43**, 72 (2005).
[27]S. E. Feller and A. D. MacKerell, J. Phys. Chem. B **104**, 7510 (2000).

[28]J. B. Klauda, B. R. Brooks, A. D. MacKerell, R. M. Venable, and R. W. Pastor, J. Phys. Chem. B **109**, 5300 (2005).
[29]W. L. Jorgensen, and J. D. Madura, Mol. Phys. **56**, 1381 (1985).
[30]HyperChem 7, Hypercube Inc., Florida, 2002.
[31]O. N. de Souza and R. L. Ornstein, Biophys. J. **72**, 2395 (1997).
[32]L. D. Landau and M. E. Lifshitz, *Statistical Physics*, 3rd ed. (Butterworth-Heinemann, Oxford, 1996).
[33]A. Bondi, J. Chem. Phys. **68**, 441 (1964).
[34]T. J. Richmond, J. Mol. Biol. **178**, 63 (1984).
[35]U. Essmann, L. Perera, M. L. Berkowitz, T. Darden, H. Lee, and L. Pederson, J. Chem. Phys. **103**, 8577 (1995).
[36]Sh. Miyamoto and P. Kollman, J. Comput. Chem. **13**, 952 (1992).
[37]H. J. Berendsen, J. P. Postma, W. F. van Gunsteren, A. DiNola, and J. R. Haak, J. Chem. Phys. **81**, 3684 (1984).
[38]G. A. Jeffrey, *An Introduction to Hydrogen Bonding*, Topics in Physical Chemistry (Oxford University Press, New York, 1997).
[39]W. B. Lee, R. Mezzenga, and G. H. Fredrickson, Phys. Rev. Lett. **99**, 187801 (2007).
[40]W. B. Lee, R. Mezzenga, and G. H. Fredrickson, J. Chem. Phys. **128**, 074504 (2008).
[41]D. T. Cromer and J. B. Mann, Acta Crystallogr. Sect. A: Cryst. Phys. Diffr. Theor. Gen. Crystallogr. **24**, 321 (1968).